Implementation of a material model for TRIP-steels in LS-DYNA and comparison with test results

Daniel Hilding(*) and Erik Schedin(**)

2002-10-31

(*) Engineering Research Nordic AB, Garnisonen, Brigadgatan 16, 581 31 Linköping, daniel.hilding@erab.se

(**) AvestaPolarit AB, Avesta Research Centre, 774 80 Avesta, erik.schedin@avestapolarit.com

Abstract

This paper describes the implementation of a new material model into LS-DYNA version 960, LSTC (1-4), a material model capable of predicting the TRIP-effect of HyTensX for different forming operations in different temperature scenarios.

The implementation is verified by comparing measurements from three tension tests with simulations of the tension tests. The comparison shows good to excellent agreement, which is a strong indication that the implementation is correct and that the material model can be used to predict the hardening behavior of the material with good accuracy.

Introduction

The driving forces to decrease weight of components have increased dramatically in recent years. New legislations concerning fuel consumption and emission from vehicles are perhaps most important. There are several ways to minimize the weight of a component. The first idea is probably to choose a so-called lightweight material like aluminium, plastic or magnesium. However, limitations in mechanical properties and fabrication techniques for these materials often make it more efficient to choose steel as the lightweight material. The method is then to choose ultra high strength steel and minimize the weight through the chosen gauge and an adapted product design. None of these two approaches can be stated as better or worse in general. It is all about the demands on the final component and design philosophy, although designs in ultra high strength steel in many cases yield the lowest weight.

The traditional ultra high strength steel approach, with ultra high strength in as-received condition, is limited by the fact that available forming methods become fewer with increasing material strength. To overcome this limitation AvestaPolarit has developed and patented a method called TensForm – where the material gains ultra high strength levels through the shaping operation and the normal limitations in formability of high strength material are eliminated.

TensForm utilises the extreme TRIP-effect of the material HyTensX (TRIP = Transformation Induced Plasticity). In this material, a phase transformation from austenite to martensite occurs during forming, an effect which is sensitive not only to the strain level, but also to temperature and strain rate. The TensForm method gives new possibilities to design for strength. The strength level can be generated where it is needed, instead of having it all over the component. In order to fully utilise the TensForm approach, it is necessary to develop simulation techniques to predict the strength level after a certain forming operation and also, to optimise a certain design from a strength level approach. It is also necessary to be able to predict the service behavior of the final component.

This paper describes the implementation of a new material model into LS-DYNA version 960, LSTC (1-4). The material model is capable of predicting the TRIP-effect of HyTensX for different forming operations in different temperature scenarios. A comparison to experimental data is presented.

Material model

Not many research groups have worked on FE-simulation of the TRIP-effect. Most published works has been on so-called isothermal models, ie, material models describing the material behavior at a fixed temperature. However, real forming operations are not isothermal, instead they are highly non-isothermal and due to the fact that the TRIP-effect is sensitive to the thermal history, a non-isothermal approach is necessary to adopt. The latter non-isothermal approach is used in Hänsel et al. (5) and verified for austenitic stainless steel of type 1.4301.

Hardening rule by Hänsel et al. (5)

This section contains a short description of the hardening model by Hänsel et al. The notation of the original work is used as much as possible. The model is composed of two basic equations to describe the TRIP-kinetics. First the martensite rate equation, equation 12 in Hänsel et al. (5),

$$\frac{\partial V_m}{\partial \varepsilon} = \frac{B}{A}\exp(Q/T)\left(\frac{1\text{-}V_m}{V_m}\right)^{(B+1)/B}\left(V_m\right)^p \frac{1}{2}(1-\tanh(C+DT)) . \qquad \text{(Eq. 1)}$$

The martensite fraction is integrated from eq. 1

$$V_m = \int_0^{\varepsilon} \frac{\partial V_m}{\partial \varepsilon} d\varepsilon \ .$$

The yield stress is, equation 16 in Hänsel et al. (5),

$$\sigma_y = (B_{HS}\text{-}(B_{HS}\text{-}A_{HS})\exp(\text{-}m\varepsilon^n))(K_1 + K_2 T) + \Delta H_{\gamma\to\alpha'} V_m , \qquad \text{(Eq. 2)}$$

where

ε = effective plastic strain,

V_m = martensite volume fraction $0.0 < V_m \leq 1.0$,

T = temperature,

σ_y = yield stress.

There is in total 13 material parameters in Eq. 1 and 2: A, B, Q, p, C, D, B_{HS}, A_{HS}, m, n, K_1, K_2, and $\Delta H_{\gamma\to\alpha'}$. In addition, the initial Martensite fraction V_{m0} is also a parameter.

Note that if V_m = 0.0 then the martensite rate is zero, i.e. the initial martensite volume fraction V_{m0} must be set to a non-zero value or else no martensite will be formed. The following conditions should be fulfilled by the parameters in the hardening rule:

1. (1+B)/B<p, if not fulfilled then the martensite rate will approach infinity as V_m approaches zero.
2. n>1.0, if not fulfilled the hardening modulus will approach infinity as the plastic strain approaches zero.

Changes to the material model in the implementation

In the implementation two minor additions to the original formulation of the yield criteria by Hänsel et al. (5) are made. These are described in the following.

Modification of hardening rule

To avoid the restriction implied by condition 2 in Section 2.1, a parameter ε_0 has been added to eq. 2 to obtain

$$\sigma_y = (B_{HS}\text{-}(B_{HS}\text{-}A_{HS})\exp(-m\varepsilon^n + \varepsilon_0))(K_1 + K_2 T) + \Delta H_{\gamma\rightarrow\alpha} V_m, \quad \text{(Eq. 3)}$$

Setting the parameter ε_0 larger than zero, typical range 0.001-0.02, leads to that n<1.0 does not imply that the hardening modulus will approach infinity as the plastic strain approaches zero. Further, the parameter K_2 is not included in the implementation as it is usually set to zero. This means that the temperature effect on the hardening of the austenitic phase is neglected.

Alternate yield surface

In Hänsel et al. (5) a von Mises yield surface with isotropic hardening is used. In the present implementation the anisotropic planar yield surface by Barlat and Lian (6) is used.

Implementation

The Hänsel material model is implemented as a user-defined material in LS-DYNA and is written in Fortran. The implementation of the Barlat and Lian (6) yield surface follows Brännberg (7).

A simple pseudo Euler backwards algorithm is used to integrate the rate equations. For large-scale simulations, an implementation of the material model using a more advanced return-mapping algorithm could reduce the simulation time significantly.

Coupled thermal analysis

LS-DYNA uses a so-called staggered step technique to perform the coupled mechanical/thermal analysis. Temperatures at the integration points are provided by LS-DYNA for the user material subroutine. The plastically dissipated energy is transformed to heat automatically by LS-DYNA, i.e. it is not necessary to do this in the user-material routine.

The simulation should be performed using an absolute temperature scale, e.g. Kelvin, when using Hänsel et al. hardening.

Verification of the material model

Tension test

A simulation of three tension tests have been performed with the dual purpose of:

1. Evaluate the ability of the material model to predict the tension test results.
2. Verify the material subroutine with respect to implementation errors.

The material was HyTensX from Avesta Polarit AB.

Identification of material parameters

The methodology worked out by Hänsel et al. was adopted, comprised by tensile testing at a constant ram speed to a preset strain level and then unloading. The temperature and martensite content were recorded during the whole tensile test, including unloading. The martensite content was recorded with a ferritoscope mounted on the specimen with a specially designed fixture and the temperature was measured with a K-type thermocouple fixed to the tensile sample with a clothes peg in wood. In the post processing of data, the influence of ferritescope readings on sheet thickness and stress level was compensated for with a special procedure.

Six tension tests were performed with varying ram speed and starting temperature. Different histories of temperature, martensite volume fraction, and true stress as a function of plastic strain where obtained from these tests. The material parameters in the material model were identified through a least squares fit of the true stresses predicted by the material model to the true stresses measured in the 6 tension tests. The obtained parameters are given in Table 2.

Examples of the result of the fitting procedure are shown in Fig 1 and Fig 2. As can be seen, a very good fit to experimental data was obtained for the martensite transformation. For the flow stress curve, the fit is acceptable, even if the result could have been better for small strains. Work to improve the material model is on going.

Table 1 Performed tensile tests.

Experiment #	Test velocity (mm/s)	Initial temperature (°C)	Lankford parameter (r-value)	Initial thickness (mm)
1	0.95	26.5	1.38	0.97
2	0.95	27.7	1.30	0.98
3	0.47	26.1	1.28	0.97
4	0.47	24.9	1.26	0.97
5	0.09	-2.0	1.20	1.00
6	0.09	2.4	1.07	1.01

Table 2 Identified material parameters, notation according to eq(1) and eq(3).

A	B	C	D (1/K)	p	Q (K)	K_2
0.32	0.226	-2.173	0.0084	6.25	1379.4	0.0
ε_0	A_{HS} (N/mm^2)	B_{HS} (N/mm^2)	m	n	$\Delta H_{\gamma\to\alpha'}$ (N/mm^2)	V_{m0}
0.002	318.2	2170	2.94	1.39	414.7	0.0001
K_1						
1.0						

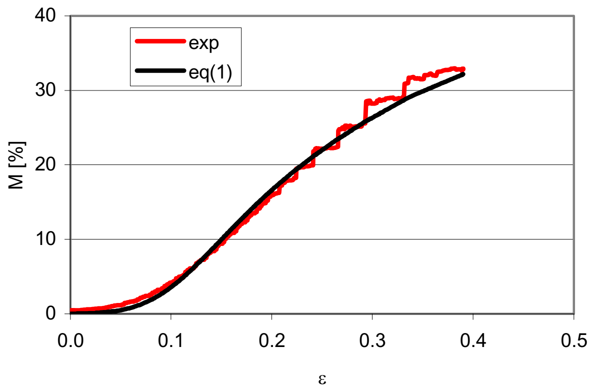

Fig 1

Comparison between eq(1) and experimental data for the martensite transformation.

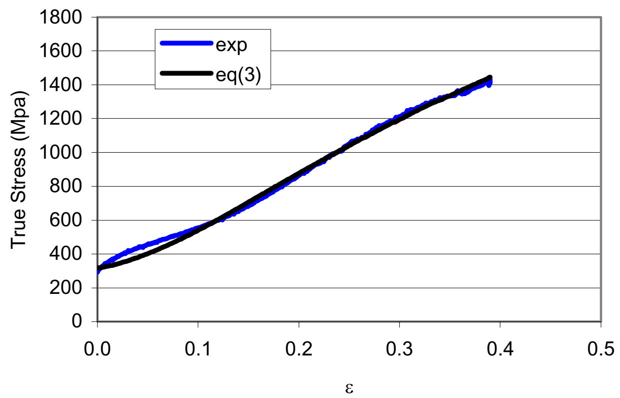

Fig 2

Comparison between eq(3) and experimental data for the flow stress.

Thermal and mechanical properties not identified from the tests

In lack of test data, several physical parameters values typical for stainless steel have been used. These are given in Table 3. The Barlat exponent was set to 6, as recommended for steel (the Lankford parameters are set to the value as given in Table 1 for each experiment).

No measurements of the thermal boundary conditions where done, instead the values given for a similar test situation in Hänsel et al. (5) was used, see Table 4.

The clamps grip the specimen 45 mm into the specimen head and across the entire width. It is assumed that the clamps have a constant temperature equal to the room temperature, which is 20 °C. The thermal efficiency was set to 90% as a general rule of thumb. The thermal efficiency is the amount of plastic dissipative energy converted to heat.

Table 3 General physical properties.

Density	7800 kg/m^3
Young's modulus	210 GPa
Poisson's ratio	0.3
Heat capacitivity	460 J/(kg K)
Thermal conductivity	25 W/m^{2}K

Table 4 Thermal boundary conditions from Hänsel et al. (5).

Heat transfer coefficient to external air	25 W/m^{2}K
Heat transfer coefficient to clamping	3000 W/m^{2}K

Simulation

The simulations where performed using explicit time integration with LS-DYNA 960. Linear Belytschko-Tsay finite elements (B-T) were used. In LS-DYNA, the B-T element is the most common choice for forming simulations. The finite element mesh is pictured in Fig 3. Simulations where performed only of tension tests number 1, 3, and 5, as the remaining tests where duplicates of the mentioned three tests.

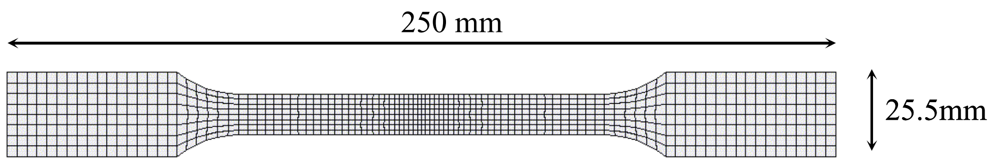

Fig 3 Finite element mesh used in the simulation.

Results

The test results where post-processed using LS-POST, LSTC (3). The temperature, plastic strain, effective stress, martensite volume fraction, and thickness were recorded in the geometric center of the test coupon. From the recorded results curves describing the temperature, effective stress, martensite volume fraction, and thickness, as a function of plastic strain are calculated. Examples of these results together with the results from the experimental tensile test are given in **Fehler! Verweisquelle konnte nicht gefunden werden.**. Note that all stress and strain results are reported in true stress and true (logarithmic) plastic strain.

Comments to the results

The simulation of the measurements from the tension tests show good to excellent agreement for all recorded results: temperature, martensite, stress, and thickness, see **Fehler! Verweisquelle konnte nicht gefunden werden.**. There are however, some important deviations, which indicate some necessary improvements of the simulation methodology and material model.

The temperature increase is well predicted up to a strain level of approximately 0.3. Then, the rate of increase for the experimental data levels off while the simulations predict a stable rate from zero strain. If the temperature curve is studied in detail it can be seen that it resembles a logarithmic growth rather than the parabolic growth predicted by simulations. The reason for the deviation is not known, but it seems reasonable that it is due to the fact that HyTensX is austenitic when the test starts and then turns into a more and more ferritic material as the test continues. Due to this, the thermal parameters for austenite should be gradually changed during the test. It is well known that a ferritic material is not heated as much during forming as an austenitic material and this should be taken into account in the simulations.

In spite of the errors in temperature predictions, the TRIP-effect is fairly well predicted. However, this is true for the strain levels achieved in tensile testing. Probably, this would not be as convincing for higher strain levels where the martensite content would be higher and the temperature more over estimated.

The flow stress curve, which is the most important end-result of the simulation, is well predicted for all of the tensile tests. There is a slight indication from the results, that the flow stress curve might not be as well predicted at higher strains than obtained in tensile testing. The deviations of the flow stress at small strains are not due to simulation accuracy, but to imperfections in the way the material model itself can describe the flow stress, as shown in Fig 2.

Fig 4 Comparison between simulations and experiments for tensile testing of HyTensX with a starting temperature at room temperature.

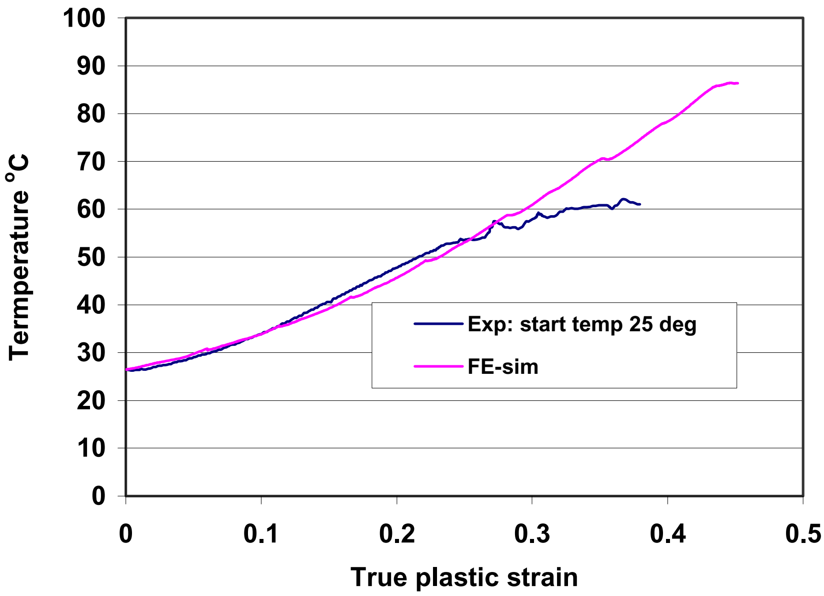

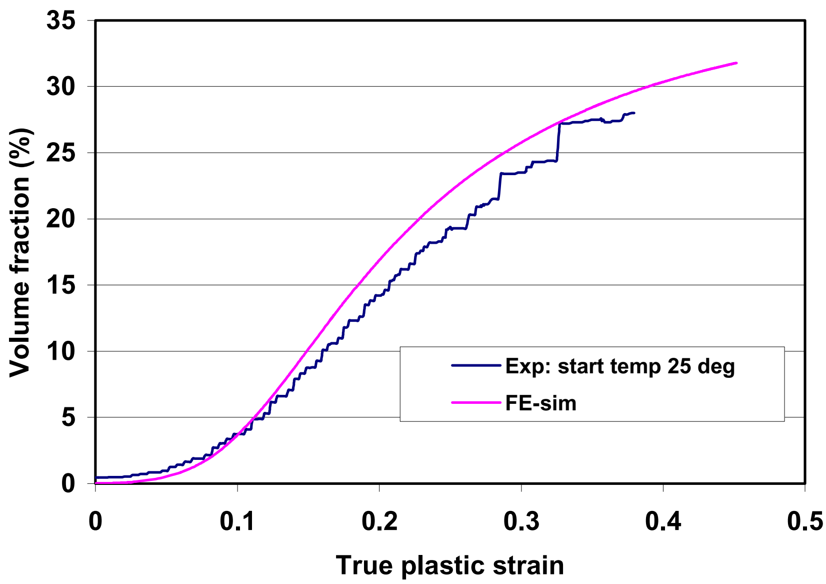

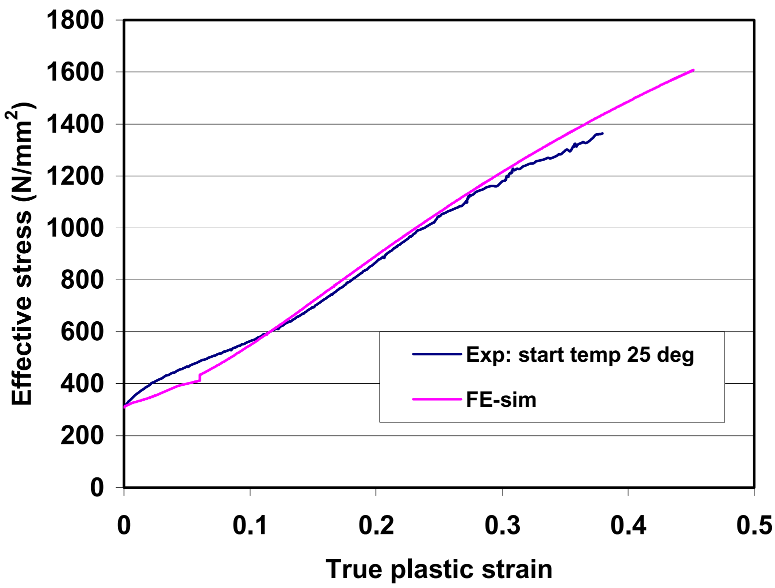
Effective stress (N/mm2)
1800
1600
1400
1200
1000
800
600
400
200
0
0
0.1
0.2
0.3
0.4
0.5
True plastic strain
Exp: start temp 25 deg
FE-sim

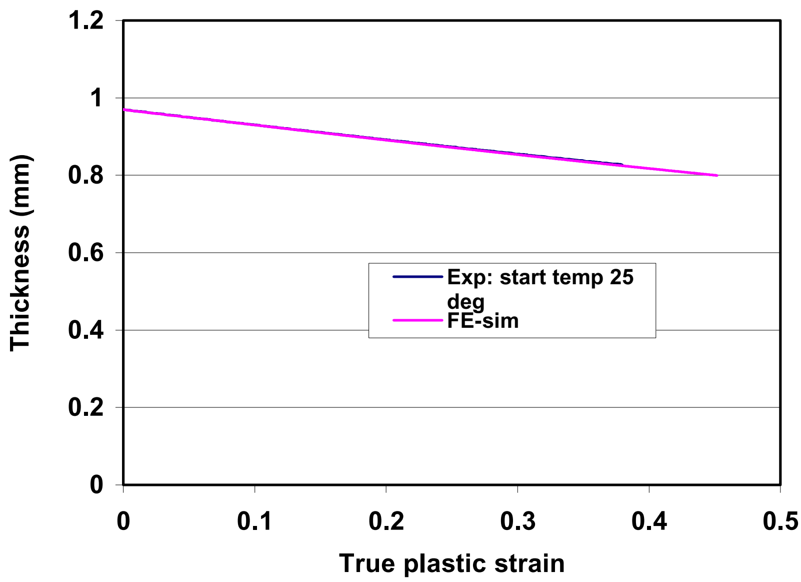
Thickness (mm)
1.2
1
0.8
0.6
0.4
0.2
0
0
0.1
0.2
0.3
0.4
0.5
True plastic strain
Exp: start temp 25 deg
FE-sim

Conclusion

The implementation is verified by comparing measurements from three tension tests with simulations of the tension tests. The comparison shows good to excellent agreement, which is a strong indication that the implementation is correct and that the material model is able to predict the hardening behavior of the material with good accuracy.

References

(1) LS-DYNA Keyword User's Manual, version 960 Volume I, Livermore Software Technology Corporation, Livermore, 2001.

(2) LS-DYNA Keyword User's Manual, version 960 Volume II, Livermore Software Technology Corporation, Livermore, 2001.

(3) LS-PRE/POST Manual, Livermore Software Technology Corporation, Livermore, 2002.

(4) LS-DYNA Theoretical Manual, Livermore Software Technology Corporation, Livermore, 1998.

(5) A. H. C. Hänsel, P. Hora, and J. Reissner, "Model for the kinetics of strain-induced martensitic phase transformation at non-isothermal conditions for the simulation of sheet metal forming processes with metastable austenitic steels", Simulation of Materials Processing: Theory, Methods, and Applications, Huétink and Baaijens (eds), Balkema, Rotterdam, 1998.

(6) F. Barlat and J. Lian, "Plastic behavior and stretchability of sheet metals. Part 1: A yield function for orthotropic sheets under plane stress conditions", Int. J. of Plasticity 5, 51.66, 1989.

(7) N. Brännberg, Computational Aspects of Simulation of Sheet Metal Forming, Ph.D thesis, Division of Solid Mechanics, Linköping university, Linköping, 1994.